Table I. Medium Effects on the Neutral Hydrolysis of **1** in Dilute Aqueous Solutions of Monosaccharides[a] at 25.0 ± 0.1 °C

carbohydrate[a]	dominant conformation[b]	G(C),[c] J·kg·mol^{-2}	G(CHOH,endo),[d] J·kg·mol^{-2}	$K°_2$(s) × 10^4,[e] cm^3·mol^{-1}·bar^{-1}
2a, D-glucose	1e2e3e4e6e	−201 (12)	−45	−17.8 (0.3)[f]
2b, D-galactose	1e2e3e4a6e	−142 (11).	−31	−20.8 (0.5)[f]
2c, D-mannose	1a2a3e4e6e	−227 (12)	−52	−16.0 (0.5)[f]
2d, D-allose	1e2e3a4e6e	−228 (15)	−52	
2e, D-talose	1a2a3e4a6e	−280 (10)	−65	−11.9 (0.3)
3a, D-fructose	1e2a3e4e5a	−202 (12)	−45	−21.6 (0.4)
3b, L-sorbose	1e2a3e4e5e	−212 (23)	−49	−21.8 (0.4)
4a, D-xylose	1e2e3e4e	−253 (18)	−52	−12.9 (0.5)[f]
4b, L-arabinose	1a2e3e4a	−129 (10)	−21	−19.3 (0.5)[f]
4c, D-lyxose	1a2a3e4e	−241 (18)	−49	−13.1 (0.1)
4d, D-ribose	1e2e3a4e	−223 (10)	−45	−12.5 (0.2)[f]

[a] 0–1.00 mol·kg^{-1}. [b] Axial (a) or equatorial (e) position of OH is indicated. [c] Experimental value. [d] Calculated from experimental data assuming that G(−0−) = 91.8 J·kg·mol^{-2} and G(CH$_2$) = −136 J·kg·mol^{-2}; e.g., G(D-glucose) = 4 × G(CHOH,endo) + G(CHOH,exo) + G(−0−) + G(CH$_2$). [e] Isentropic partial molar compressibility. [f] Reference 18.

coefficient of water (Φ = 1 for m_c = 0), and G(C) depicts the overall effect of the carbohydrate on the Gibbs energy of activation for the hydrolytic process.[15] Excellent straight lines were obtained by plotting ln ($k_{obsd}/k°_{obsd}$) vs m_c, and the G(C) values calculated from the slopes of these lines are listed in Table I. Some representative plots are shown in Figure 1.

All carbohydrates cause a rate retardation which is quantitatively expressed in the negative G(C) values. Interestingly, these G(C) values are almost invariant for many of the hexoses and pentoses and do not respond to the presence of a keto- or aldohexose, the anomer distribution, and the number of equatorial OH groups in the molecule.[16] A significantly different G(C) is only found when the OH at C-4 is axial (e.g., D-galactose, D-talose, and L-arabinose), but the effect depends on the relative orientation of the next nearest neighbor,[17] the OH moiety at C-2. When OH(4) and OH(2) are trans toward each other, G(C) is markedly less negative, for the corresponding cis orientation G(C) is markedly more negative (Table I). In fact, the G(C) value for D-talose is even more negative than that for the relatively hydrophobic monohydric alcohol 1-propanol (−258 ± 6 J·kg·mol^{-2}),[13] indicating that D-talose is recognized by the hydrolytic probe as a relatively hydrophobic solute.

On the next level of sophistication, one can calculate group interactions[14] for the overall effect of the carbohydrate on the Gibbs energy of activation. The calculations were performed for the pyranose form, which is the dominant conformer in aqueous solution. From the difference in G(C) between hexoses and pentoses one obtains G(CHOH,exo) = +25 J·kg·mol^{-2}, a value comparable to that found for a similar group in vicinal dihydric alcohols.[13] Now G(CHOH,endo) values (Table I) can be calculated. These are all negative, which means that intermolecular interactions of these groups lead to rate retardation and are, therefore, dominated by the methine moieties in the endocyclic CHOH function. We note that the limiting isentropic compressibilities of the carbohydrates[18] (Table I), which are a measure of the water compatibility of the solute,[19] follow the same trends as the G(CHOH,endo) values. Taken together, these results indicate that the better the carbohydrate fits into the three-dimensional hydrogen-bond structure of water, the more the OH groups are camouflaged[20] for interaction with the kinetic probe and the more negative G(CHOH,endo) is found.

We gather from the present results that the carbohydrates can be classified into three groups in order of decreasing hydration and diminished fit into the water structure: (1) both OH(2) and OH(4) are axial (D-talose); (2) OH(4) is equatorial and OH(2) is either axial or equatorial (**2a**, **2c**, **2d**, **3a**, **3b**, **4a**, **4c**, and **4d**); (3) OH(4) is axial and OH(2) is equatorial (D-galactose and L-arabinose). Our results suggest that molecular recognition in aqueous carbohydrate solutions is probably governed by an interplay between the rigid polyol structure of the carbohydrate, dictated by its detailed stereochemistry, and the flexible three-dimensional hydrogen-bond structure of water, apt to respond to subtle structural variations in a solute. Additional studies are underway aimed at further modeling of the stereochemical aspects of carbohydrate hydration in aqueous solution.

Acknowledgment. These investigations were supported by the Netherlands Foundation for Chemical Research (SON) with financial aid from the Netherlands Foundation for Scientific Research (NWO). We are indebted to Prof. F. Franks for stimulating discussions and to Mr. G. J. Gerwig (University of Utrecht) for his help in product analyses (GC and GC/MS). Limiting compressibilities were measured in the Chemistry Department of the University of Bergen, Norway. We thank Prof. H. Høiland for his hospitality.

(15) Careful analysis of the reaction mixtures by GC (Varian 3700 instrument) and combined GLC/MS (Carlo-Erba GC/Kratos MS80/Kratos DS 55 system) revealed the absence of carbohydrate-derived esters. Full experimental details will be given in a full paper.

(16) The presence of furanose forms also hardly affects the G(C) values since similar trends are found for a series of methyl pyranosides.

(17) Warner, D. T. *Nature* **1962**, *196*, 1055.
(18) Høiland, H.; Holvik, H. *J. Solution Chem.* **1978**, *7*, 587.
(19) Cesaro, A. In *Thermodynamic Data for Biochemistry and Biotechnology*; Hinz, H. J., Ed.; Springer: Berlin, 1986; Chapter 6.
(20) Franks, F.; Ravenhill, J. R.; Reid, D. S. *J. Solution Chem.* **1972**, *1*, 3.

Template-Synthesized Polyacetylene Fibrils Show Enhanced Supermolecular Order†

Wenbin Liang and Charles R. Martin*

Department of Chemistry, Colorado State University Fort Collins, Colorado 80523

Received September 17, 1990

We have recently described the synthesis of nanoscopic fibrils of heterocyclic polymers.[1] These fibrils were synthesized via a template method, in which the pores in a nanoporous membrane act as templates for the nascent polymer. Such fibrils show electronic conductivities (along the fibril axis) which are substantially higher than conductivities of bulk films of the analogous polymer.[1] We suggested that this enhanced conductivity resulted from preferential orientation of the polymer chains parallel to the fibril axis;[1] however, we had no experimental data to support this contention.

This paper provides experimental proof for such enhanced supermolecular order in template-synthesized conductive polymer fibrils. We describe (for the first time) the template synthesis of nanoscopic polyacetylene fibrils. We then present results of a polarized infrared absorption experiment which prove that the polyacetylene chains in these fibrils are preferentially oriented

* Corresponding author.
† Part of this work was conducted when the authors were at Texas A&M University.

(1) Cai, Z.; Martin, C. R. *J. Am. Chem. Soc.* **1989**, *111*, 4138.

0002-7863/90/1512-9666$02.50/0

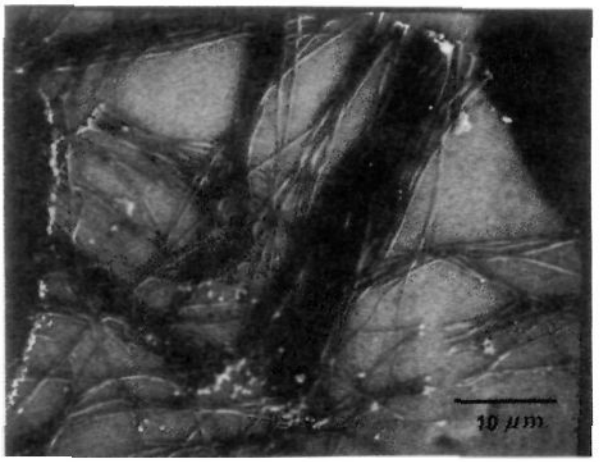

Figure 1. Scanning electron micrograph of template-synthesized polyacetylene fibrils.

parallel to the fibril axis. Finally, we show that these fibrils have higher electronic conductivities than polyacetylene film synthesized under identical conditions. These studies provide the first example of preferential chain orientation in a conductive polymer without postpolymerization processing or synthesis in a liquid crystal solution.[2]

Fibrils were synthesized by polymerizing acetylene within the pores (diameter = 200 nm) of an Anopore[3] filtration membrane. The polymerization catalyst was $Ti(OBu)_4/AlEt_3$.[4] The Anopore membrane and catalyst solution were added to the polymerization vessel (a septum-sealed glass tube). The catalyst solution was impregnated into the pores of the host by evacuating the vessel, heating to 70 °C, and then back-filling with Ar. The excess catalyst was removed with a syringe. The vessel was then evacuated again, and acetylene gas[5] was introduced. Polymerization was allowed to proceed for 2 h, at 0 °C.[6] The membrane was then washed in sequence with degassed toluene, 5% HCl in methanol, and pure methanol and then dried in vacuo.

Figure 1 shows a scanning electron micrograph of the polyacetylene fibrils. This micrograph was obtained by dissolving the Anopore membrane[3] and then collecting the fibrils by filtration. The fibrils show good monodispersity of both length and diameter; this is a characteristic feature of the template method.

The polarized infrared absorption (PIRA) experiment[7] was conducted on the Anopore–polyacetylene composite membrane. (Leaving the fibrils embedded in the Anopore membrane insured that all of the fibrils were oriented in the same direction in space.) The composite membrane was positioned at an angle of 45°[8] with respect to the incident beam of the spectrometer.[9] A gold wire grid polarizer was used to control the angle of polarization of the incident beam. The absorbance of the composite membrane by

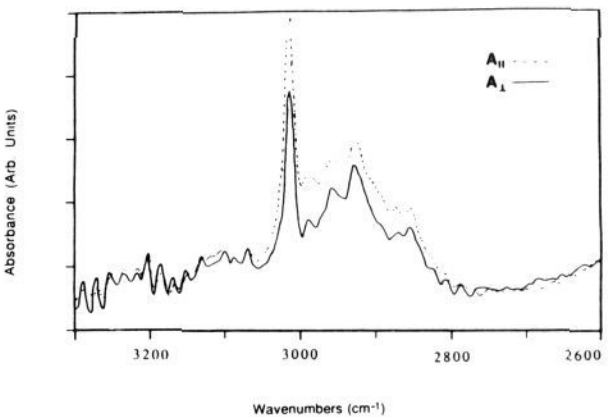

Figure 2. Polarized infrared absorption spectra (in the C–H stretching region) for an Anopore membrane/polyacetylene fibril sample. $A_{\parallel}$ and $A_{\perp}$ are absorbances parallel[8] and perpendicular to the fibril axis.

radiation polarized perpendicular and parallel[8] to the fibril axes was measured (Figure 2).

Polyacetylene was chosen for these studies because analogous PIRA investiigations have been conducted on stretched polyacetylene film.[2] Stretching causes preferential orientation of the polyacetylene chains parallel to the stretch axis, and the effects of this preferential orientation on the PIRA spectra have been well documented.[2] These investigations serve as reference points for the data obtained in this study.

PIRA spectra for the C–H stretching mode in the polyacetylene fibrils are shown in Figure 2.[10] In analogy to the stretch-oriented material,[2] the fibrils preferentially absorb light polarized parallel to the fibril axis. The dichroic ratio, R,[7] can be obtained from the PIRA spectra ($R = A_{\parallel}/A_{\perp}$, where $A_{\parallel}$ and $A_{\perp}$ are the integrated absorption intensities for light polarized parallel[8] and perpendicular, respectively, to the fibril axes).

An R value of 1.46 was obtained from the spectra in Figure 2, indicating that the polymer chains in these fibrils are preferentially oriented (see below). It is important to point out that virgin Anopore membrane shows $R = 1.0$ (no orientation). Furthermore, when the composite membrane is oriented at an angle of 90° relative to the incident beam, $R = 1.0$ is also obtained; this is expected because this 90° orientation insures that the vectors for both polarizations are normal to the fibril axes. These studies serve as controls for the data in Figure 2.

A quantitative picture of the supermolecular structure in these fibrils can be obtained by calculating the average orientation angle (θ) between the polymer chains and the fibril axis.[7] This calculation requires a value for R and for the angle (α) between the transition moment of the vibration and the axis of the polymer chain.[7] Investigations of stretch-oriented polyacetylene[2] have shown that $\alpha = 48°$ for the C–H stretching mode. The orientation angle can vary from $\theta = 90°$ (polymer chains oriented perpendicular to the fibril axis) to $\theta = 0°$ (chains oriented parallel to the axis). A θ value of 22.5° is obtained for the polyacetylene fibrils, indicating a high degree of *parallel* orientation.

If the polymer chains are, indeed, oriented parallel to the fibril axis, then conductivity along this axis should be enhanced.[1,2] Conductivity along the fibril axis was measured by using the method described in ref 1; p-doped samples were investigated.[11] A conductivity of 1425 S cm^{-1} was obtained. Conventional polyacetylene film, synthesized and doped under identical conditions, showed a conductivity of 325 S cm^{-1}. Thus, the parallel polymer chain orientation does, indeed, yield enhanced electronic conductivity along the fibril axis.

We have shown that template synthesis yields enhanced supermolecular order and higher electronic conductivities in con-

(2) (a) Aldissi, M. *J. Polym. Sci., Polym. Lett.* **1989**, *27*, 105. (b) Castiglioni, C.; Zerbi, G.; Gussoni, M. *Solid State Commun.* **1985**, *56*, 863.
(3) Van Dyke, L. S.; Martin, C. R. *Langmuir* **1990**, *6*, 1118.
(4) Naarmann, H.; Theophilou, N. *Synth. Met.* **1987**, *22*, 1.
(5) Acetylene (99.6%, Scott) was purified by passage through concentrated H_2SO_4 and a column of activated alumina.
(6) As was observed previously,[1] template synthesis yielded conductive polymer fibrils running through the membrane and thin polymer films covering both faces of the membrane. These surface layers were peeled from the membrane faces.
(7) (a) Monnerie, L. In *Developments in Oriented Polymers*; Ward, I. M., Ed.; Elsevier: London, 1987; Vol. 2, p 199. (b) Zbinden, R. *Infrared Spectroscopy of High Polymers*; Academic Press: New York, 1964; p 166.
(8) The ideal geometry for these measurements would be to impinge the light onto the edge of the membrane so that the parallel polarization would be truly parallel to the axes of the fibrils. This is not possible because the membranes are only 55 μm thick. For this reason the 45° geometry was adopted. In this geometry, the polarization vector for the "parallel" component is *coplanar* with the axis of the fibril but intersects the fibril at an angle of 45°. Thus, only a component of the "parallel" polarization is truly parallel to the fibril axis. The effects of this geometrical arrangement were accounted for[7] in the determination of the orientation angle (θ).
(9) An IBM IR/30 FTIR spectrometer was used.
(10) Undoped polyacetylene shows only a few distinct IR bands.[2] These other bands are buried beneath the Anopore absorption.
(11) Shirakawa, H.; Louis, E. J.; MacDiarmid, A. G.; Chiang, C. K.; Heeger, A. J. *J. Chem. Soc., Chem. Commun.* **1977**, 578.

ductive polymers. We are currently developing a mechanistic model for this enhanced order. We are also exploring the extent to which other types of polymers can be ordered via the template method. Template synthesis may prove to be a general procedure for obtaining highly ordered nanoscopic polymeric fibrils.

Acknowledgment. This work was supported by the Office of Naval Research and the Air Force Office of Scientific Research.

Structure of Pyrrolosine: A Novel Inhibitor of RNA Synthesis, from the Actinomycete *Streptomyces albus*

Susumu Ikegami,* Haruhiko Isomura, and Noboru Tsuchimori

Faculty of Applied Biological Sciences Hiroshima University, Kagamiyama Higashihiroshima-shi, Hiroshima 724, Japan

Yasuko T. Osano, Tetsuro Hayase, Tomoko Yugami, Haruyuki Ohkishi, and Takao Matsuzaki

Research Center, Mitsubishi-Kasei Corp. Kamoshida-cho, Midori-ku, Yokohama-shi Kanagawa 227, Japan

Received August 24, 1990

During the last 20 years, our knowledge of the biosynthesis of RNA has expanded greatly, due largely to the discovery and use of various inhibitors of RNA synthesis. Several inhibitors of RNA synthesis have been used as anticancer, antiviral, and antibacterial agents.[1] However, there are very few, if any, specific inhibitors of RNA synthesis without undesirable side effects on cellular functions. We have searched for microbial products capable of arresting the development of starfish embryos specifically at the early blastula stage, when RNA synthesis becomes active, without interfering with cell division at the morula stage or with blastula formation, which are independent of RNA synthesis.[2] We encountered a culture broth conditioned by the actinomycete *Streptomyces albus* A282, which showed marked activity in the starfish assay and which led us to isolate the active component. Now we report the structure elucidation of the active constituent, pyrrolosine.

The culture broth filtrate (17 L) was passed through a column of Diaion HP-20.[3] The absorbed material was eluted with MeOH. The eluate was subjected to low-pressure column chromatography on silanized silica gel (H_2O/5% MeOH), then alumina (70% MeOH), and finally Robar RP-8[4] (10% MeOH), to give pyrrolosine (**1**) (246 mg) as colorless plates, $[\theta]_{240}$ +2300° (*c* 0.0014, MeOH). Pyrrolosine (10 μg/mL) inhibited RNA synthesis of starfish (*Asterina pectinifera*) embryos at blastulation and halted embryonic development just after completion of blastulation. Furthermore, pyrrolosine inhibited cell growth of transformed human fibroblast KMST-6 cells and mouse mammary carcinoma FM3A cells at IC_{50} 13 and 27 ng/mL, respectively. The molecular formula of $C_{11}H_{13}N_3O_5$ was established by an MH^+ ion peak at *m/z* 268 in the FAB mass spectrum and by elemental analysis. Pyrrolosine showed UV absorption maxima [$\lambda_{max}^{H_2O}$ (pH 7.0) 220 (ε 10000), 242 (4400), 272 nm (4200); (pH 1.5) 225 (5800), 268 (7500 sh), 276 (7800), 285 nm (5200 sh)]. ^{13}C NMR spectra[5] revealed 11 carbon signals, five of which are assignable to a ribosyl unit. Detailed 270- and 400-MHz NMR analyses[6] including H-H COSY[7] and C-H COSY experiments[8] (^1J and long range) suggested strongly that the structure of pyrrolosine is 7-(β-ribofuranosyl)-4-oxo-3*H*,5*H*-pyrrolo[3,2-*d*]pyrimidine. This *C*-nucleoside analogue of inosine was reported as having been synthesized and was designated 9-deazainosine by Lim et al.[9] However, HPLC analysis (Radialpak NVC18,[10] 0.8 × 10 cm; 20% MeOH) revealed that the retention volume of 9-deazainosine[11] was 2.9 mL whereas that of pyrrolosine was 3.8 mL. Furthermore, the UV spectrum[12] of 9-deazainosine was different from that of pyrrolosine. Therefore, the structure of pyrrolosine was deduced by single-crystal X-ray diffraction. Repeated crystallization from a mixture of MeOH and ethyl acetate afforded colorless hexagonal plates (methanol monosolvate; mp 105–110 °C) belonging to the orthorhombic space group $P2_12_12_1$ with a = 9.994 (1) Å, b = 19.441 (1) Å, c = 7.026 (1) Å, and Z = 4. Intensities were measured in the ω–1.33θ scan mode on an Enraf-Nonius CAD4 diffractometer, using graphite-monochromated Cu Kα radiation (λ = 1.5418 Å). Correction was made for Lorentz and polarization factors but not for absorption. Of 1655 independent reflections measured in a range of $2° < 2\theta < 149°$, 31 reflections with $|F_o| < 1.0\sigma(|F_o|)$ were considered unobserved.

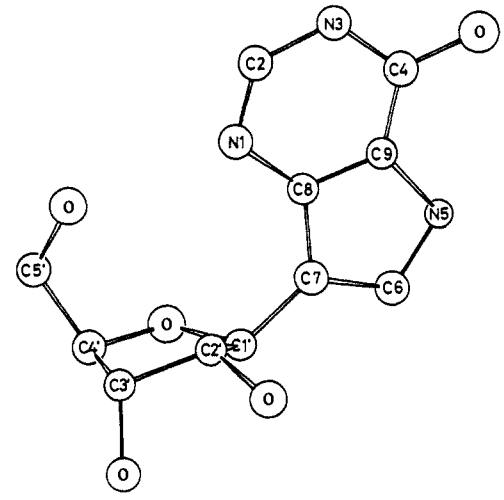

Figure 1. Computer-generated perspective drawing of pyrrolosine. Hydrogens are omitted for clarity, and no absolute configuration is implied.

The structure was determined by direct methods coupled with the MULTAN 11/82 program.[13] Its parameters were refined by the full-matrix least-squares method using anisotropic temperature factors for non-hydrogen atoms. The final R value for 1624 reflections used in the refinement process was 0.065. A computer-generated perspective drawing of the final X-ray model of pyrrolosine (**1**) is given in Figure 1. The X-ray experiment did not define the absolute configuration, so the enantiomer shown is arbitrary. The structure of pyrrolosine is the same as that proposed for synthetic 9-deazainosine.

Synthetic "9-deazainosine" was shown to be toxic in vitro to protozoan cells but not to mammalian cells.[14] Starfish embryos developed normally in the presence of the reputed "9-deazainosine"

(1) Sung, S. C. *Life Sci* **1974**, *15*, 359–369.
(2) Isomura, H.; Itoh, N.; Ikegami, S. *Biochim. Biophys. Acta* **1989**, *1007*, 343–349.
(3) Mitsubishi-Kasei Corp., Tokyo, Japan.
(4) E. Merk, Darmstadt, West Germany.
(5) ^{13}C NMR (D_2O, 67.8 MHz): δ 62.9 (t, C-5'), 72.7 (d, C-3'), 75.6 (d, C-2'), 76.4 (d, C-1'), 86.2 (d, C-4'), 119.3 (s), 135.3 (s), 147.2 (s), 149.4 (d, C-6), 150.6 (s, C-4), 153.1 (d, C-2).
(6) ^1H NMR (D_2O, 270 MHz): δ 3.84 (2 H, br AB q, J = 14.0 Hz, H-5'), 4.22 (1 H, br m, H-4'), 4.32 (1 H, br d, J = 7.2 Hz, H-3'), 4.52 (1 H, dd, J = 7.4 and 7.2 Hz, H-2'), 5.04 (1 H, d, J = 7.4 Hz, H-1'), 8.02 (1 H, s, H-6), 8.15 (1 H, s, H-2).
(7) Bax, A.; Freeman, R. *J. Magn. Reson.* **1981**, *44*, 542–561.
(8) Morris, G. A.; Hall, L. D. *J. Am. Chem. Soc.* **1981**, *103*, 4703–4714.
(9) Lim, M.; Klein, R. S.; Fox, J. J. *Tetrahedron Lett.* **1980**, *21*, 1013–1016.
(10) Waters Assoc., Milford, MA.
(11) Generous gift of Dr. Robert S. Klein, Memmorial Sloan-Kettering Cancer Center Walker Laboratory, Rye, NY.
(12) $\lambda_{max}^{H_2O}$ (pH 7.0) 230 (ε 16600), 260 nm (5900).
(13) Main, P.; Fiske, S. J.; Hull, S. E.; Lessinger, L.; Germain, G.; Declercq, J.-P.; Woolfson, M. M. *MULTAN 11/82, a system of computer programs for the automatic solution of crystal structures from X-ray diffraction data*; University of York: York, England, 1982.
(14) LaFon, S. W.; Nelson, D. J.; Berens, R. L.; Marr, J. J. *J. Biol. Chem.* **1985**, *260*, 9660–9665.

0002-7863/90/1512-9668$02.50/0